THE ASTROPHYSICAL JOURNAL SUPPLEMENT SERIES, 131:335–353, 2000 November

XID: CROSS-ASSOCIATION OF *ROSAT*/BRIGHT SOURCE CATALOG X-RAY SOURCES WITH USNO A-2 OPTICAL POINT SOURCES

ROBERT E. RUTLEDGE, ROBERT J. BRUNNER, AND THOMAS A. PRINCE
Division of Physics, Mathematics and Astronomy, MS 220-47, California Institute of Technology, Pasadena, CA 91107;
rutledge@srl.caltech.edu, rb@astro.caltech.edu, prince@srl.caltech.edu

AND

CAROL LONSDALE
Infrared Processing and Analysis Center, Caltech/JPL, Pasadena, CA 91125; cjl@ipac.caltech.edu
Received 1999 December 8; accepted 2000 April 4

ABSTRACT

We quantitatively cross-associate the 18,811 *ROSAT* Bright Source Catalog (RASS/BSC) X-ray sources with optical sources in the USNO A-2 catalog, calculating the probability of unique association (P_{id}) between each candidate within 75″ of the X-ray source position, on the basis of optical magnitude and proximity. We present catalogs of RASS/BSC sources for which $P_{id} > 98\%$, $P_{id} > 90\%$, and $P_{id} > 50\%$, which contain 2705, 5492, and 11,301 unique USNO A-2 optical counterparts respectively down to the stated level of significance. Together with identifications of objects not cataloged in USNO A-2 due to their high surface brightness (M31, M32, …) and optical pairs, we produced a total of 11,803 associations to a probability of $P_{id} > 50\%$. We include in this catalog a list of objects in the SIMBAD database within 10″ of the USNO A-2 position, as an aid to identification and source classification. This is the first RASS/BSC counterpart catalog which provides a probability of association between each X-ray source and counterpart, quantifying the certainty of each individual association. The catalog is more useful than previous catalogs which either rely on plausibility arguments for association or do not aid in selecting a counterpart between multiple off-band sources in the field. Sources of high probability of association can be separated out, to produce high-quality lists of classes (Seyfert 1/2s, QSOs, RS CVns) desired for targeted study, or for discovering new examples of known classes (or new classes altogether) through the spectroscopic classification of securely identified but unclassified USNO A-2 counterparts. Low P_{id} associations can be used for statistical studies and follow-on investigation—for example, performing follow-up spectroscopy of the many low-mass stars to search for signatures of coronal emission, or to investigate the relationship between X-ray emission and classes of sources not previously well-studied for their X-ray emissions (such as pulsating variable stars). We find that a fraction $\sim 65.8\%$ of RASS/BSC sources have an identifiable optical counterpart, down to the magnitude limit of the USNO A-2 catalog which could be identified by their spatial proximity and high optical brightness.

Subject headings: catalogs — X-rays: general

On-line material: machine-readable tables

1. INTRODUCTION

The *ROSAT* Bright Source Catalog (BSC; Voges et al. 1996, 1999) contains positions, X-ray count rates, and spectral information of 18,811 X-ray sources with count rates greater than 0.05 counts s^{-1}, observed during the *ROSAT* All-Sky-Survey (RASS).

Efforts to identify the sources of X-ray emission with counterparts in other wavebands are hampered by source confusion. The error region of the RASS/BSC sources average $\sim 12''(1\ \sigma)$, which can contain several candidate objects, any of which may be the source of X-rays.

To date, most efforts to identify the X-ray sources with parent populations—usually, optical sources—have been targeted toward subgroups of known X-ray emitting populations, such as coronal X-ray sources (Berghoefer et al. 1997; Huensch, Schmitt, & Voges 1998a, 1998b; Huensch et al. 1999) AGNs/QSOs (Thomas et al. 1998; Beuermann et al. 1999) OB stars (Berghoefer et al. 1996, 1997; Motch et al. 1997a, 1997b) and high Galactic latitude spectrally soft sources (Thomas et al. 1998). As part of a larger effort to identify QSOs, a general spectroscopic survey has also identified stellar type sources (Bade et al. 1995, 1998).

Many of these associations—though not all—have been based upon an argument of plausibility. In the plausibility method, one typically performs imaging photometry and spectroscopy of objects within the X-ray error box and finds a plausible counterpart among these; a counterpart is usually considered plausible if the candidate object's class is previously known to emit X-rays, and if the properties (such as magnitude, or implied L_X/L_{opt}) are consistent with those previously observed from other objects within its class. This method is useful when the parent population is known and rare (much less than one object per average X-ray error box size). However, this method will not discover X-ray sources independent of object classification. In addition, some of the studies which rely upon plausibility do not measure the level of background contamination, while others do not evaluate the limiting P_{id} (the lowest probability of unique identification a prospective counterpart can have, and still be included in the catalog). None provide a P_{id} for each cross-identification, which makes it impossible to quantitatively evaluate the quality of a purported association in future work.

In Table 1, we list previous works which catalog $\gtrsim 100$

TABLE 1

PUBLISHED RASS/BSC COUNTERPART CATALOGS ($N \gtrsim 100$)

Reference	Cross-ID Catalog	N_{src} (N_{bkg} = %)	Criteria for ID	Limiting Significance[a]
1.....	Stars (AFGKM; I through III–IV); From Yale BSC (Hoffleit & Jaschek 1991)	450 (21.8 = 4.8%)	<90″ from X-ray source	$R > 50\%$
2.....	Stars (AFGK class IV, V and subtypes) From Yale BSC	980 (21.8 = 2.2%)	<90″ from X-ray source	$R > 50\%$
3.....	Nearby Stars (Gliese & Jahreiss 1991)	1252 (24 = 1.9%)	<90″ from X-ray source	$R > 50\%$
4.....	RASS/BSC: Medium-bright, Spectrally soft, $\|b\| > 40°$ Optical/spectral survey	75 (n/a)	Plausibility	n/a
5.....	OB stars in the Yale BSC	216 (0.5 = 0.23%)	<45″ from X-ray source	n/a
6.....	RASS/BSC: Bright (>0.5 counts s^{-1}), Spectrally soft (HR1 < 0), $\|b\| > 20°$	397 (n/a)	Plausibility	n/a
7.....	Cygnus: $86° < l < 94°$, $-5° < b < 5°$	128 (2 = 1.5%)	Plausibility	$R > 98\%$
8.....	Full Sky, optical/spectral survey	3847 (<9 = 0.2%)	Plausibility	n/a
9.....	*HST*-GSC	9759 (1358 = 13.92%)	<24″ from X-ray source	$R > 50\%$
Present work.....	USNO A-2, *B* objects	2705 (18 = 0.7%)	$P_{id} \geq 98\%$ (see text)	$P_{id} \geq 98\%$
Present work.....	USNO A-2, *B* objects	5492 (155 = 2.8%)	$P_{id} \geq 90\%$ (see text)	$P_{id} \geq 90\%$
Present work.....	USNO A-2, *B* objects	11301 (2034 = 18%)	$P_{id} \geq 50\%$ (see text)	$P_{id} \geq 50\%$

[a] At the limit of the catalog—previous work used *R* (eq. [10]), which does not include probability of source confusion; present work uses P_{id}, which does include probability source confusion (eq. [5]).

REFERENCES.—(1) Huensch et al. 1998a; (2) Huensch et al. 1998b; (3) Huensch et al. 1999; (4) Beuermann et al. 1999; (5) Berghoefer et al. 1996, 1997; (6) Thomas et al. 1998; (7) Motch et al. 1997a, 1997b; (8) Bade et al. 1995, 1998; (9) Voges et al. 1999.

optical counterparts to RASS/BSC objects, or which sought RASS/BSC counterparts for a particular class of sources. The table includes: (1) the reference; (2) brief description of the cross-identification catalog; (3) the number of cross-identifications found and the estimated number of mis-identified (background) sources in the cross-ID list (N_{bkg}); (4) a brief description of the identification algorithm used; (5) and the probability of unique association (P_{id}) between the X-ray source and candidate counterpart at the identification limit of the catalog.

For several of these works, no estimation of the probability of cross-identified sources being background sources at the detection limit was given. Of those which do, a probability of confusion with background (that is, unassociated) sources of $\sim 50\%$ is a common limit (below which, the identified counterpart is more likely to be an unrelated background object than actually associated with the X-ray source). An extensive comparison with several published and unpublished cross-identification catalogs was made in Table 3 of the RASS/BSC work (Voges et al. 1999) (for a total of $\sim 17{,}000$ sources), which we discuss more completely in § 5. We include, for comparison, the results of the present work.

We have undertaken a project of off-band identification of *ROSAT*/BSC X-ray sources—XID. The goal of this project is to provide a catalog of cross-identifications, which provides the probability of unique identification (P_{id}) between the off-band counterpart for all RASS/BSC sources.

We have additional motivation for performing the present work. Future databases of sources—both in the X-ray and in other bands—will and already do contain 10^5–10^9 objects. This is too great a number of objects on which to perform nonautomated methods for identifying counterparts. We therefore develop and use an automated method for identifying cross-band counterparts, which can be further adapted and used in future studies.

We present the method and results of a statistical cross-identification between RASS/BSC and USNO A-2 catalogs, producing a high-, medium-, and low-quality cross-identification list. We summarize these results and provide a short discussion on the content of the cross-identification catalog. These catalogs are given in the Appendix.

2. METHOD

2.1. *Data Selection*

We began with the full *ROSAT* Bright Source Catalog (Voges et al. 1999, hereafter V99), of 18,811 X-ray sources. We use the source name, position (R.A. and decl.), and positional uncertainty. For 57 of these sources, the catalog positional uncertainty was given as 0″, for various reasons specific to the source detection algorithms; we adopt, for these objects, positional uncertainties of 30″. This makes up our X-ray source list.

We extracted from the USNO A-2 catalog,[1] the positions and *B* magnitudes of all those sources which were within 75″ of the X-ray source positions. These sources make up the cross-identification candidate list, the contents of which are (1) the name of the RASS/BSC source; (2) the positional uncertainty of the RASS/BSC source in arcsec; (3) the name of the candidate USNO A-2 object; (4) the distance between the RASS/BSC and USNO A-2 source positions in arcsec; (5) and the *B* magnitude of the USNO A-2 object.

We also extracted from the USNO A-2, for each X-ray source field, ten background fields, each 75″ in radius. These background fields were offset in R.A. from the X-ray source position, by $n \times 150''$, for $n = [-5, -1]$ and $n = [1, 5]$, five to the east and five to the west. These sources make up the background list.

In Figure 1, we compare the distributions in *B* magnitude, between the cross-identification list and the background list. There is a clear excess of objects in the source fields at $B < 17$, indicating associated optical sources in this magnitude range. There is a deficit of objects at faint magnitudes ($B > 20$). We can think of no astronomical reason

[1] http://ftp.nofs.navy.mil/projects/pmm/a2.html.

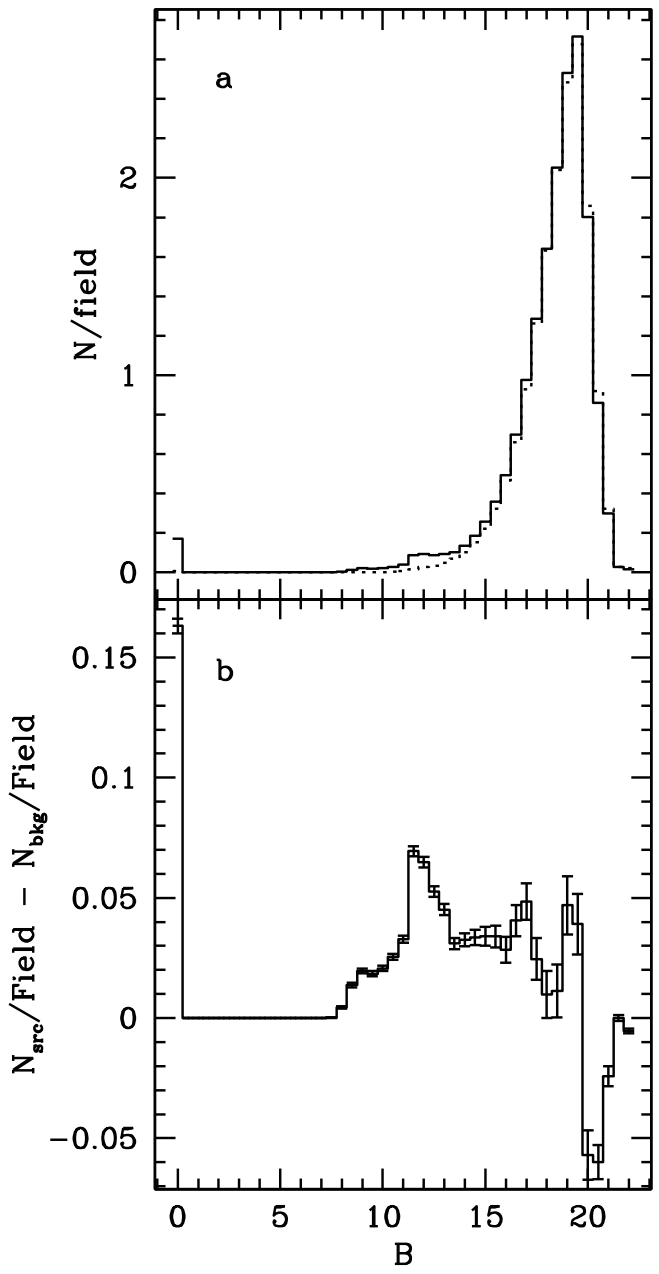

FIG. 1.—Comparison between cross-identification catalog objects (*solid line*) and background field catalog objects (*broken line*). (*a*) Distributions of *B* magnitude. (*b*) Difference between distributions in *B* magnitude.

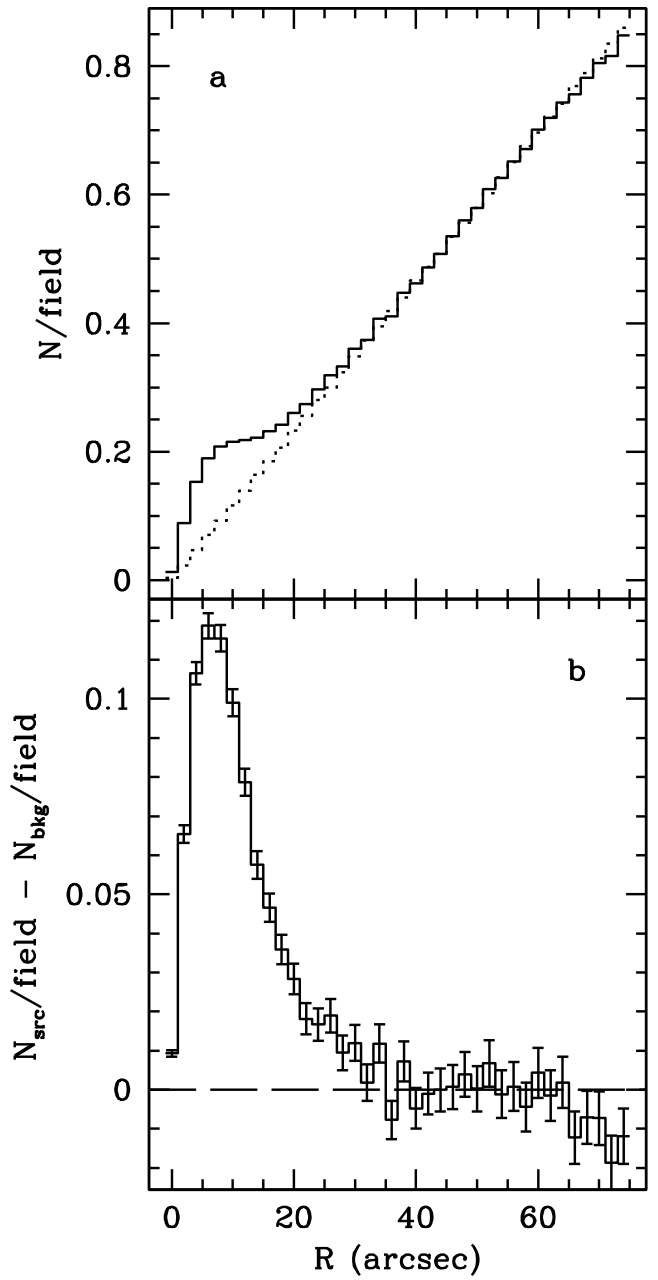

FIG. 2.—Comparison between cross-identification catalog objects (*solid line*) and background field catalog objects (*broken line*). (*a*) Distributions in distance between X-ray source position and optical source. (*b*) Differences between distributions shown in panel *a*.

why there might be fewer faint optical objects in our source fields, but we have found that, in fields which contain bright objects ($B < 14$), there are fewer faint objects ($B > 18$) than in fields which do not contain such bright objects; it therefore seems likely that the deficit of faint objects in our source fields are due to the excess of bright objects. As our method is tuned to select for the brightest objects in the field, this will not affect our results.

In Figure 2, we compare the distribution between the field center and optical objects for source fields (where the X-ray position is the field center) and background fields (where there is no X-ray source at the field center). There is an excess of objects in X-ray source fields within 20″ of the X-ray source position, and no excess of sources at greater separations. Thus, there is a tendency for there to be bright objects in close positional association with the X-ray sources, simply through comparison of the optical object characteristics in source fields and background fields.

2.2. *Method of Calculating of the Probability of Unique Association* (P_{id})

The applied method of cross-association is based on a method described elsewhere (Lonsdale et al. 1998). This method is similar to one previously employed (Sutherland & Saunders 1992 and references therein), but handles systematic uncertainties in the measured source characteristics through statistical comparison between "on-source" and background fields, whereas these previous methods

assumed perfect knowledge of source characteristics. We here repeat essential parts of this method, expanding upon particular modifications of the original method as used in the present application.

We begin with the catalog of N_X X-ray sources. We consider for each X-ray source the M candidate USNO A-2 objects in the cross-identification catalog. For the ith counterpart candidate, we calculate a likelihood ratio—a likelihood of association between the optical object and the X-ray source—through a specified likelihood ratio method (LR), which we take to be like a product of probabilities:

$$LR_i = \Pi_j P_j(x_i) , \quad (1)$$

where P_j is a normalized probability distribution of some property x of the ith counterpart candidate. The functions P_j can be—in principle—any function of the properties x_i; however, the results depend intimately upon the form of the functions chosen, so they must be considered carefully. By selecting functions P_j which are ratios of the a priori distributions of true counterparts to distributions of background sources, the product LR_i has a number of useful properties. Most importantly, LR will be high (on average) for true counterparts and low (on average) for background sources. This permits the true counterparts to cluster at high LR values, which is desirable for a reason which will become clear.

In the present case, we adopt a Gaussian distributed positional coincidence for sources and an expectation that the counterpart be very bright (low magnitude), the LR for the ith optical source is

$$LR_i = \frac{\exp - r_i^2/2\sigma_i^2}{\sigma_i N(<B_i)} , \quad (2)$$

where r_i is the distance to the USNO A-2 object from the X-ray source position in arcsec, σ_i is the uncertainty in the source positions (which we approximate in this case as the uncertainty in the *ROSAT*/BSC source position, which is 12.″7 on average, and is typically between 5″ and 25″, Gaussian distributed; Voges et al. 1999), and $N(<B)$ is the absolute number of sources in the background list with magnitude less than some value B, and B_i is the magnitude of the ith source (in the present comparison, we use the USNO A-2 B magnitude).

The LR value is calculated for objects in the source fields and the background fields. Following this, we calculate a reliability R of identification as a function of likelihood ratio:

$$R(LR_i) = \frac{N_{\rm true}(LR_i)}{N_{\rm true}(LR_i) + N_{\rm false}(LR_i)} , \quad (3)$$

which is the ratio of the number of true associations to the sum of the true and false associations, as a function of the LR of those identifications. $R(LR_i)$ is the binomial probability that a optical/X-ray source pair with a specific value of LR is a true association and that the optical source is not an unrelated background source. This is the probability which some previous catalogs (cf. Table 1) quote as the limiting probability.

The probability R does not, however, include the probability that another object in the field of view could instead be the counterpart—that is, while the probability R of an X-ray/optical pair does state the probability of association, it may well be that there are other sources in the field of view which are just as likely to be an association. In other words, the X-ray/optical association is not *unique*.

We now calculate (1) the probability that a particular X-ray source has no associated optical source in the USNO A-2 catalog ($P_{\rm no\text{-}id}$), and (2) the probability that an optical source i is the *unique* association with the X-ray source ($P_{\rm id,i}$).

For a particular RASS/BSC X-ray source, there will be M USNO A-2 objects under consideration as the possible *unique* association, for which we have already calculated M probabilities (R) for association between the X-ray source and each optical source. We now impose a set of $M + 1$ exclusive and complete hypotheses and calculate probabilities of these hypotheses being true, using the probability of X-ray/optical associations R. The hypotheses are

Hyp. i ... M.—The ith optical source is uniquely associated with the X-ray source, and none of the other X-ray sources are associated ($P_{\rm id,i}$).

Hyp. $M+1$.—None of the M optical sources are uniquely associated with the X-ray source ($P_{\rm no\text{-}id}$).

Since $R(LR_i)$ is the binomial probability that the ith object is associated with the X-ray source, the probability that *none* of the M objects are associated with the X-ray source is

$$P_{\rm no-id} = \frac{\Pi_{j=1}^{M}(1 - R_j)}{S} , \quad (4)$$

where S is a normalization, specific to each X-ray source, which we define below. The probability that the X-ray source, then, has an optical counterpart in the USNO A-2 catalog is $1 - P_{\rm no\text{-}id}$.

For each X-ray source in the source catalog, the probability of the association with the ith optical source is

$$P_{\rm id,i} = \left[\frac{R_i}{1 - R_i}\,\Pi_{j=1}^{M}(1 - R_j)\right] \Big/ S \quad (5)$$

(S, again, is defined below). This is the product of the probability (R_i) that the ith optical object is associated with the X-ray source and is not a background source, and the probability that all other $j(\neq i)$ optical sources in the field are *not* associated with the object and are background sources.

The quantity S is a normalization specific to each X-ray source such that the $M + 1$ hypotheses form a complete set: $P_{\rm no\text{-}id} + \Sigma_{i=1}^{M} P_{\rm id,i} = 1$:

$$S = \Sigma_{i=1}^{M} \frac{R_i}{1 - R_i}\,\Pi_{j=1}^{M}(1 - R_j) + \Pi_{j=1}^{M}(1 - R_j) . \quad (6)$$

$P_{\rm id,i}$, $P_{\rm no\text{-}id}$ are now defined as functions dependent only upon values of $R(LR)$. Since $P_{\rm id,i}$ and $P_{\rm no\text{-}id}$ are dependent only upon the sums and products of $R(LR)$, they too will converge as $R(LR)$ does, according to the central limit theorem.

For each ith optical source, the value $P_{\rm id,i}$ is always less than $R(LR_i)$. This is because there can be more than one (even, many) optical source with a high value of R associated with an X-ray source, but the set of hypotheses above excludes the possibility that more than one of these is associated with the X-ray source (for example, binary stellar systems, galaxy clusters, or many bright optical sources in nearby open clusters).

Finally, we can calculate the "quality" of an association catalog, which we denote by Q:

$$Q = \langle 1 - P_{\text{no-id}} \rangle . \quad (7)$$

The value of Q is the fraction of the initial X-ray catalog which has an association in the cross-ID optical catalog. It is dependent only on the presence of potential counterparts in the USNO A-2 catalog.

It is possible to formulate an approach in which more than one optical source is associated with the X-ray source, and we apply one approach (for binary systems) in § 2.4. However, this can quickly become a (restrictively) computationally intensive problem, as the approach requires producing source pairs, triplets, etc., and therefore the number of combination objects grows as the combination factor (a factorial). For example, there can be 15 possible optical sources in the field of an X-ray source. To consider only a unique identification, there are only 15 data objects (the X-ray/optical pair). To consider possible binary identifications, there are $15!/(15-2)!/2! = 105$ data objects; to consider triplet identifications, there are $15!/(15-3)!/3! = 455$ data objects, and so on.

The means of quantifying the fraction of sources which do not fit exactly into the unique association/no association hypotheses is through S (eq. [6]). S is the sum of all probabilities in the unique association/no association hypotheses, and therefore, the average value of S (over all X-ray sources) is the average probability that one of the $M + 1$ hypothesis is satisfied; $1 - S$ is then the probability that none of the hypotheses are satisfied. See § 3.3 for the quantitative estimation of $\langle 1 - S \rangle$.

The values and meaning of R and P_{id} are different and should be viewed differently. The value of R is the binomial probability of association between the X-ray source and the USNO A-2 object—or of any USNO A-2 object of that B magnitude and the same angular distance from the X-ray source. It is possible that more than one USNO A-2 source in the same field have high reliability (e.g., $R = 0.999$). This could occur for example, if a counterpart is one star of a binary of equal magnitude; or if the counterpart is a star in a crowded open cluster, and in which there may be many examples of similarly optically bright sources; or if the plate-scanning detection algorithm finds a saturated star and does not correctly subtract all the flux, leaving residuals in which a second "star" is found. Thus, while a high value of R does mean the source is unusual in background fields (and therefore probably associated with the X-ray source) it does not account for confusion—the fact that any number of sources in the field can have similarly high R, due to astronomical or systematic considerations. By calculating P_{id} (eq. [5]), we find the probability that a particular object is associated and that *none of the other objects in the field* are associated. In this way, P_{id} accounts for confusion, while R does not. Note that in all cases, $P_{\text{id}} \leq R$.

2.3. *Practical Calculation of the Probabilities*

After defining the probabilities above, we now go about estimating them. The sum of the number of true associations and false associations (cf. eq. [3]) is the total number of objects (per field) in source fields, with the value LR:

$$N_{\text{true}}(LR) + N_{\text{false}}(LR) = N_{\text{source}}(LR) . \quad (8)$$

We also observe the number of false associations as the total number of objects (per field) in background fields with the value LR:

$$N_{\text{false}}(LR) = N_{\text{background}}(LR) . \quad (9)$$

Using these observed quantities, we estimate the reliability as a function of LR:

$$\tilde{R}(LR) = \frac{N_{\text{source}}(LR) - N_{\text{background}}(LR)}{N_{\text{source}}(LR)} , \quad (10)$$

where we use $\tilde{R}(LR)$ to indicate the calculated approximation of $R(LR)$ (eq. [3]). In calculating $\tilde{R}(LR)$ it is necessary to generate sufficient numbers of objects so that the uncertainty in values of $N(LR)$ is small, and so that $\tilde{R}(LR)$ will converge according to the central limit theorem. We used LR bin-sizes of $\log LR = 0.5$ (full width), in a running sum, centered around the source LR value, except at the high and low ends of the LR distribution, where we used a single LR bin between the highest value of $\log LR$ and $\log LR - 0.5$. If we found that the bin-size was insufficient to establish $\tilde{R}$ to better than 0.01 (assuming Gaussian counting statistics) or there were fewer than 1000 sources (from the source field) in a bin, we doubled the bin-size until there were sufficient numbers of objects to meet this criterion. Finally, $\tilde{R}(LR)$ should be a monotonically decreasing function of LR for low values of LR (where background sources dominate). We chose to set $\tilde{R}(LR) = 0$ for all values $LR < LR_0$, where LR_0 is the greatest value where $\tilde{R}(LR) = 0$. This is equivalent to removing from analysis the candidate associations which are considered unlikely counterparts according to our criteria. In the present analysis, $\log LR_0 = -10.31$.

In Figure 3, we show the calculated LR and R values upon which the identifications are made. In the top panel, there is an excess of sources with high LR in the on-source fields compared to the background fields. As per equation (10), this excess of sources at high LR produces the high reliability for these objects (*lower panel*). The excesses are *statistical*—it is the fact that there are excesses in significant numbers above that expected from background fields which produces secure identifications.

We then assign the estimated $\tilde{R}(LR)$ to the X-ray/optical pairs of value LR. From these $\tilde{R}$-values, we estimate the probability of unique association according to the method in § 2.2.

To estimate the uncertainty in the resulting P_{id} (where we have suppressed the subscript i for brevity) and $P_{\text{no-id}}$, we propagate the uncertainty in the *background* objects, taken to be small and Gaussian, which is a reasonable assumption under the conditions that the LR bin from which $\tilde{R}$ is calculated has either $N_{\text{source}}(LR) \gg N_{\text{background}}(LR)$ or $N_{\text{background}} \geq 100$, which for all our bins in the present analysis is true. We show in our results section the estimated uncertainty in P_{id}, as a function of P_{id}.

We applied three different probability criteria, to produce three catalogs of different quality: $P_{\text{id}} \geq 98\%$, $98\% > P_{\text{id}} \geq 90\%$, and $90\% > P_{\text{id}} \geq 50\%$.

2.4. *Identifying Binary Counterparts*

In some cases, there may be two or more potential counterparts in the source field, for which the calculated reliability is high, but the P_{id} is low. This will occur if, for

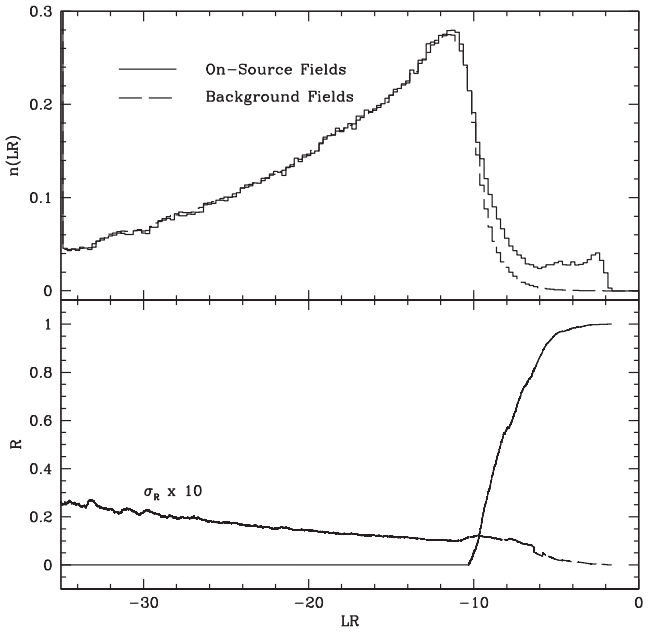

FIG. 3.—*Top*: Distribution of calculated *LR* values for RASS/BSC-USNO A-2 candidate cross-identifications in on-source fields (*solid line*) and in background fields (*broken line*)—$n(LR)$, which is number of objects per field per *LR* bin. Note the excess of such sources at $LR > -10$, indicating optical–X-ray associations. *Bottom*: Reliability—$R(LR)$ (eq. [10])—can be thought of as the probability that the optical source under consideration is *not* a background source, that it is associated with the X-ray source.

example, the counterpart is a bright ($B = 3.0$) binary. Both resolved stars could have high reliabilities (say, 0.9999), but the $P_{\rm id}$ for both would be close to 0.5; either may be the counterpart, but the algorithm above places high $P_{\rm id}$ only when the source is unlikely to be a background object, *and when there are no other sources in the field which also are unlikely to be a background object*, the latter condition being violated in the case of a bright binary pair.

One possible, but flawed, solution to this problem is to use the reliability as the indicator of a counterpart. However, this does not take into account the likelihood of finding a bright source near another bright source—such as occurs in open clusters, or in binaries. A second flawed approach is to use the values found for *R* to calculate the probability of finding two objects, each of high *R*, in a single image. However, this assumes the values of *R* to be independent which, among source fields which are clusters of objects, is not true.

Thus, we modified the above method to apply it for the special case of binaries. For each object, we first calculate a likelihood ratio for each pair in the "candidate binary counterpart" (compare with eq. [2]):

$$LR_{i,j} = LR_i \times LR_j \,. \tag{11}$$

This is done for each paired combination of sources in the source field, and in the background fields, after which, the method described for single sources applies as described above, resulting in a list of probability of identification $P_{\rm id}$ for each pair of objects in the field, a probability of no-identification $P_{\rm no\text{-}id}$ for each X-ray source (the probability of finding a binary counterparts in the field), and a *Q* value (eq. [7]). Finally, we excluded from binary-identifications those RASS/BSC sources for which a single-object identification with $P_{\rm id} > 50\%$ was already found.

2.5. *Assumptions Implicit in the Quantitative Cross-ID Method*

There are a few assumptions which are implicit in the described association method. We describe these here.

First, the method of determining the value of *LR* (eq. [1]) contains all the astronomical assumptions about the nature of the counterparts. As such, this method finds counterparts only when the observational characteristics of these counterparts are previously assumed. We have assumed that the optical counterparts will be among the brightest optical point-sources observed and that these sources are spatially coincident with the X-ray counterpart. In other applications, one might assume that a specific $f = L_{\rm X}/L_{\rm opt}$ ratio would pick out the kinds of X-ray/optical sources expected, and in that case one can fashion a *LR* method which would produce a high value of *LR* near the specified value of *f*, for example:

$$LR_i = \frac{\exp\,(-r_i^2/2\sigma_i^2)}{\sqrt{2\pi}\sigma_i} \frac{\exp\,[-(f_i - f_0)^2/2\sigma_0^2]}{\sqrt{2\pi}\sigma_0}\,, \tag{12}$$

where f_i is the ratio $L_{\rm X}/L_{\rm opt}$ of the *i*th object, f_0 is an average ratio, and σ_0 is related to the width in *f* observed sources are expected to display, and all other values are as defined for equation (2). In the method we define in equation (2). we are therefore searching for a population of counterparts which are both within the error region of the X-ray source, and which have high *B*-band fluxes. This will, quite naturally and as we intend, find a particular class of counterparts, which will therefore have these properties of spatial coincidence and optical brightness. Other classes of counterparts can be found with different definitions of *LR*.

Second, the method implicitly assumes that the properties of background objects in the source field—the brightness distribution and source density—are identical to those of the background field. This is not necessarily the case and can affect the calculated probabilities. For example, X-ray sources such as young stellar objects are often found (as we do here) in open clusters of angular size comparable to or smaller than a RASS/BSC error region. Open clusters have higher source densities than an average background field. A higher number of unrelated objects in a source field produces more sources with higher *R*, which will decrease the $P_{\rm id}$ of a particular counterpart (cf. eq. [5]). We have attempted to overcome this problem in the case of binary counterparts, by adding an analysis which will find pairs of objects; this does not address, however, counterparts with several objects in the field, such as open clusters or galaxy clusters. The means of completely overcoming this downward bias on $P_{\rm id}$ is superior X-ray localizations, which we cannot obtain for a one-of-a-kind catalog such as the RASS/BSC. Thus, this bias exists in the catalogs we present.

Third, the method demonstrates an *association* between an X-ray source and the optical counterpart—but it does not demonstrate unique *identification*. For example, if an X-ray source happens to be an optically faint galaxy in a rich galaxy cluster of an angular size comparable to or less than a RASS/BSC error region, this method will likely pick out the brightest galaxy in the cluster as the associated

object (if, indeed, the galaxy is bright enough to warrant such association), whereas the brightest galaxy is not the X-ray emitter at all. It is, however, associated with the X-ray emitter through their joint association with the cluster. Another example: the X-ray source may be hot X-ray cluster gas, which is not observed optically (at least, not in USNO A-2); again, this method will pick out the brightest galaxy in the cluster as the associated object, when it is not the X-ray source at all. Thus, systematic biases of the type where optically bright sources tend to cluster with (optically faint) X-ray sources, producing a—by our analysis—statistically significant association may very well exist in our catalog; indeed, given the known types of X-ray sources, it seems likely that they do exist in our catalog. These types of biases must be considered when interpreting the values of P_{id} assigned to an association. As an aid to evaluating these types of biases, we have included all objects in the SIMBAD databases which are within 10″ of the identified USNO A-2 counterpart.

3. RESULTS

There were 18,754 RASS/BSC objects which had 321,144 possible counterparts in a total of 24.8944 deg^2, for a source density of 12,900 $\pm$ 23 sources deg^{-2} in the counterpart catalog.

There were 57 RASS/BSC objects for which no optical sources were found in the USNO A-2 catalog within 75″ of the X-ray source position. We visually inspected the DSS survey[2] images at these locations and found that in 30 cases, the field contained a very bright, extended object (galaxies, globular clusters, or saturated star), such as M31, M82, M27, M63, or M60. Almost certainly these regions were excluded from USNO A-2 scanning due to their extended, high surface brightness emission. Although we have not quantitatively calculated their association probability, we confidently identify them as counterparts to the X-ray sources, estimating $P_{id} = 0.9998$. (We estimate this probability, assuming 1000 such objects in the sky, with average radii of 3′, which thus covers 0.02% of the total sky). For the number of RASS/BSC objects, we expect a background contamination of ~ 1. These objects are listed separately, in Table 2, along with their identification.

In other fields, there are high surface-brightness regions, likely due to nebulae or perhaps plate defects; there are some fields which appear to contain many point sources, which we would think USNO A-2 scanning should have separately found; and, there are some regions where there are clearly no detected optical point sources at all. These last make attractive fields for further study, to find optically faint/X-ray bright sources such as isolated neutron stars, distant quasars, or field LMXBs. We compile a listing of these remaining fields in Table 3. In two of these fields, no background objects were found either, although the DSS reveals a large number of suitable optical counterpart candidates, likely implying that these fields are not included in the USNO A-2 catalog.

A total of 184,446 background fields were searched, finding 301,1309 objects in the background catalog, in 244.8373 deg^2, for a source density of 12,299 $\pm$ 7 objects deg^2. This makes for a surplus of (12900 $\pm$ 23 $-$ 12299 $\pm$ 7)$*$24.8944 = 15000 $\pm$ 600 optically associated objects in the cross identification catalog, on the basis of field density alone. Since some X-ray sources are bright optical binaries, or young stellar objects associated with open clusters, or galaxy clusters, some of these excess objects are likely to be due to higher than average field densities, though it is difficult to estimate the magnitude of this effect.

In Figure 4, we show the cumulative distribution of the X-ray source probability of identification (eq. [4]). This is the probability of an individual X-ray source to have an optical counterpart among the several USNO A-2 objects within its field. There are 1184 RASS/BSC sources ($\sim 6\%$) which have at least one USNO A-2 source in the field, but which is either too faint or to distant to be considered a possible counterpart in this analysis. Approximately $\sim 39\%$ of the RASS/BSC sources have a probability of identification greater than 90%, and $\sim 67\%$ have better than a 50% probability of having an optical association within USNO A-2.

For comparison purposes, we performed the above analysis on 10% of our background fields, using them as "source fields" and comparing these to the other 90% of our background fields. In Figure 5, we show the distributions of $P_{id,i}$ for all sources within the actual source fields, compared with the $P_{id,i}$ derived from objects in the background (comparison) field. The distributions are substantially different, with no objects found with $P_{id} > 10\%$ in the comparison field. This is because (as expected) there is no significant excess number of objects found with high LR in the comparison fields over the number found in similar background fields, to the limit of the precision of the number statistics ($\lesssim 6\%$). This subsequently produces values of $R \lesssim (1.06 - 1.0)/1.06 \sim 6\%$, which is then the highest possible value of P_{id} for sources in the background field, explaining why no sources with $P_{id} > 10\%$ are found in the background field. This comparison clarifies that an

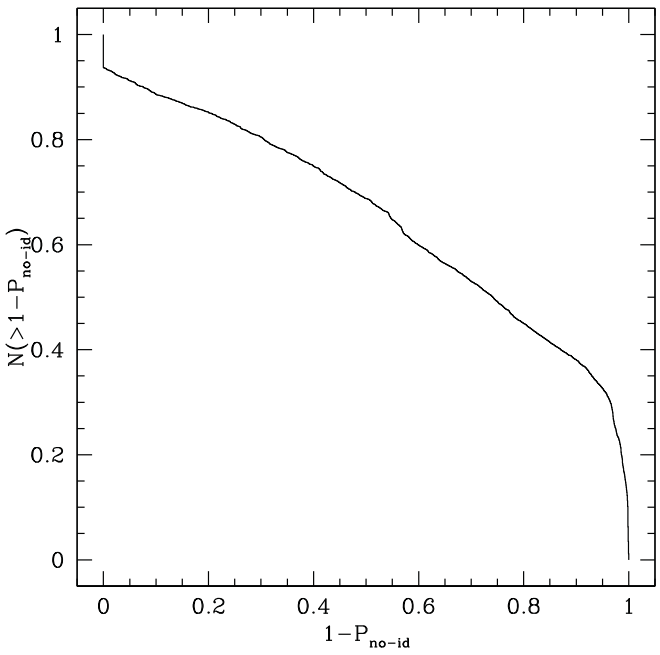

FIG. 4.—Cumulative distribution of the probability that the USNO A-2 catalog contains a cross-identification of the 18,754 RASS/BSC objects for which at least one candidate USNO A-2 object was found.

[2] http://archive.stsci.edu/dss/.

TABLE 2

BRIGHT/EXTENDED OBJECT COUNTERPARTS

1RXS	Visual Inspection	SIMBAD ID
1RXS J004241.8+411535.....	Galaxy	M31
1RXS J004733.3−251722.....	Galaxy	NGC 253 (G)
1RXS J013350.9+303932.....	Galaxy	M 33
1RXS J024620.0−301639.....	Galaxy	NGC 1097 (Sy 2)
1RXS J031819.4−662912.....	Galaxy	NGC 1313 (G)
1RXS J032241.8−371239.....	Galaxy	NGC 1316 (GiC)
1RXS J033828.8−352701.....	Galaxy	NGC 1399 (GiC)
1RXS J033851.5−353543.....	Galaxy	NGC 1404 (GiC)
1RXS J041611.4−554630.....	Galaxy	NGC 1553 (GiG)
1RXS J042000.5−545617.....	Galaxy	NGC 1566 (Sy1)
1RXS J051406.6−400234.....	Gl. Cluster	NGC 1851
1RXS J053803.8−690925.....	Galaxy	30 Doradus
1RXS J095534.7+690338.....	Galaxy	M 81
1RXS J111811.1+313154.....	Bright Sat. Binary	* 53 UMa
1RXS J112016.7+125917.....	Galaxy	M 66
1RXS J121900.4+471747.....	Galaxy	M 106 (Sy 2)
1RXS J123939.6−052035.....	Galaxy	NGC 4593 (Sy 1)
1RXS J124340.6+113309.....	Galaxy	M 60 (pair)
1RXS J125052.5+410713.....	Galaxy	M 94 (LIN)
1RXS J130528.0−492758.....	Galaxy	NGC 4945 (G)
1RXS J131549.3+420154.....	Galaxy	NGC 4945
1RXS J132527.3−430105.....	Galaxy	M 63 (G); QSO 1313+422
1RXS J132542.9−425746.....	Galaxy (offset)	M 63
1RXS J132953.8+471143.....	Galaxy	M 51/NGC 5194 (PoG)
1RXS J133657.0−295207.....	Galaxy	M 83
1RXS J134210.2+282250.....	Gl. Cluster	NGC 5272
1RXS J175012.8−370306.....	Gl. Cluster	NGC 6441
1RXS J195936.2+224309.....	PN	M 27 (Dumbbell Nebula)
1RXS J212958.4+120959.....	Gl. Cluster	M 15
1RXS J220916.6−471002.....	Galaxy	NGC 7213 (Sy 1)

NOTES.—Bright or extended objects identified by visual inspection of the DSS plate, which were originally found because there were no USNO A-2 objects listed within 75″ of the RASS/BSC position of the X-ray source. Estimated significance of the cross-identification of these objects is $P_{\rm id} = 0.999$, and they are included in the $P_{\rm id} \geq 98\%$ Catalog.

object for which $P_{\rm id} = 80\%$ (for example) does not imply that, if we were looking *only* in completely the wrong areas, there would be a 20% chance of finding a source with this $P_{\rm id}$ value.

The plateau in the source field distribution near $P_{\rm id} = 0.5$, which drops at $P_{\rm id} = 0.6$ is likely due to binary sources; a consequence of our applied method is that two very bright sources in the field, which alone would make them a likely counterpart, together mutually exclude each other.

We also investigated what would occur if we used spatial correlation alone—ignoring the brightness distribution of sources. This was done by altering the *LR* equation, to include only the component based on r and σ, and performing the analysis otherwise as described. We find zero, zero, and 5413 sources with $P_{\rm id} > 98\%$, 90%, and 50%, respectively. Compared with the 2705, 5492, and 11,301 we find when we do take B into account, this demonstrates that a substantial improvement in the statistical certainty of the identified counterpart is made when using more than just spatial information.

3.1. *The Catalogs: $P_{\rm id} \geq 98\%$ Catalog, 90% Supplementary Catalog, and 50% Supplementary Catalog*

We summarize in Table 1, along with the results of previous studies, the number of cross-identified objects in each of the 3 cumulative catalogs, the estimated number of misidentified objects, and the probability of unique association at the limit of each catalog.

We find 2705 single USNO A-2 objects with $P_{\rm id} \geq 98\%$, for an identification rate of 14.4%. Based on the probability of identification for these sources, we expect a total of $N_{\rm bkg} \sim 18$ (0.7%) are misidentified as associated with the X-ray sources. The number of misidentified sources is found:

$$N_{\rm bkg} = N - \Sigma_i P_{{\rm id},i} \, . \tag{13}$$

We searched the SIMBAD database for objects within 10″ of the identified USNO A-2 counterpart, for possible identification of these optical objects and to obtain information about the environment of the cross-identified USNO A-2 source; we provide the results of this search in the catalog tables. The 10″ radius was chosen to account for (some) proper motions of stars, and for astrometric uncertainty. This will account for stars with proper motion less than $0\farcs274\ {\rm yr}^{-1}$ comparing observational epochs 1955.0 (for the POSS I sources at declinations above −17°, as included in USNO A-2) and 1991.5.

We systematically excluded from this list the 1RXS sources themselves, although we note when a SIMBAD-listed object was also listed as the 1RXS source. These lists often include objects which are likely not the X-ray sources themselves (such as H II regions); however, including them

TABLE 3

RASS/BSC Objects with No USNO A-2 Objects $<75''$

1RXS	N Bkg Objs.[a]	Visual Inspection[b]
1RXS J000235.9−081518.....	25	(no object)
1RXS J002941.1−165408.....	26	(no object)
1RXS J004202.7−143557.....	24	(no object)
1RXS J040358.2−021113.....	29	(no object)
1RXS J052749.6−695412.....	98	Neb.
1RXS J053428.3−052414.....	8	Neb.
1RXS J053510.8−044850.....	22	Neb.
1RXS J054045.7−021119.....	25	Diff. Spike
1RXS J055054.2−621454.....	0	Many Pt Src/ Galaxy?
1RXS J055225.0−640206.....	0	Many Pt Src
1RXS J064045.4+094927.....	46	Neb.
1RXS J100407.9+144925.....	30	(no object)
1RXS J104346.4−594538.....	7	(no object)
1RXS J111005.5−763531.....	191	Neb.
1RXS J123607.4+731901.....	45	(no object)
1RXS J124601.5−680846.....	370	(no object/star?)
1RXS J124634.5−680446.....	373	(no object/star?, same as above)
1RXS J124830.1−594449.....	48	Diff. Spike?
1RXS J124849.0+333454.....	23	(no object)
1RXS J140559.3−411230.....	277	Diff. Spike
1RXS J144359.5+443124.....	42	(no object)
1RXS J153517.4−410958.....	295	Diff. Spike
1RXS J162609.7−242245.....	5	Neb./(no object)
1RXS J163910.7+565637.....	2	(no object)
1RXS J173253.6−371200.....	80	(no object)
1RXS J182102.0−161309.....	18	Neb./(no object)
1RXS J231117.9−094615.....	30	(no object)

Note.—Table contains information on fields which did not contain any USNO A-2 objects, which were then visually inspected using the DSS plate. See § 3.

[a] Total number of USNO A-2 objects in the associated background fields.

[b] Neb.—nebulosity in the field; Diff. Spike—stellar diffraction spikes in the field; (no object)—no obvious optical counterpart.

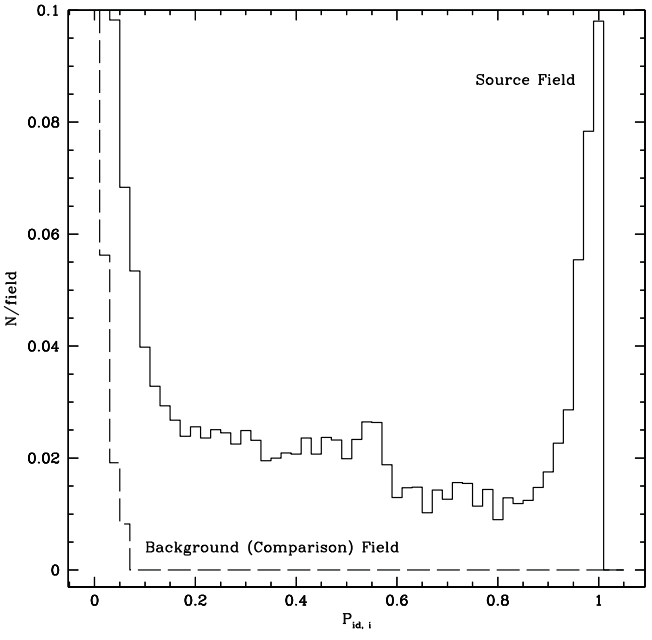

Fig. 5.—Comparison between the single-source probabilities ($P_{id,i}$) in the source fields (*solid line*) vs. in the background comparison fields (*broken line*). This comparison was performed to demonstrate what would happen if the analysis were applied to fields which are not the X-ray source fields. There are no significant excess optical sources found (up to ∼5%) at high *LR*, which limits the maximum *R* to less than (1.05–1.0)/1.05, and thus P_{id} to this value as well. The slight excess near $p = 0.5$ is possibly due to binaries in the source fields.

may help elucidate the nature of the identified USNO A-2 counterpart.

In the supplementary catalog of sources with $98\% > P_{id} \geq 90\%$ (the 90% Supplementary Catalog), we find an additional 2787 single sources, for a total $P_{id} \geq 90\%$ identification rate of 29.2%. Based on the probability of identification for these sources, a total of $N_{bkg} \sim 137$ (5.0%) of the supplementary catalog are misidentified as the counterpart to the X-ray sources; and a total of 155 (2.8%) of the combined 98% plus 90% Supplementary catalogs are misidentified as associated with the X-ray sources. This catalog, plus the $P_{id} > 98\%$ Catalog, forms the $P_{id} \geq 90\%$ Catalog.

Finally, in the supplementary catalog of sources with $90\% > P_{id} \geq 50\%$ (the 50% Supplementary Catalog), we find an additional 5809 single sources, for a total $P_{id} > 50\%$ identification rate of 60.0%. Based on the probability of identification for these sources, we expect a total of $N_{bkg} \sim 1879$ (32%) of the supplementary catalog are misidentified as the counterpart to the X-ray source. This catalog, plus the 90% Supplementary Catalog and the $P_{id} > 98\%$ Catalog, forms the $P_{id} \geq 50\%$ Catalog. While the counterparts in this catalog are of potentially useful confidence (one out of every two is the optical counterpart at the limit of the catalog, with increasing prevalence for higher P_{id}), we include these sources largely for completeness, for statistical surveys, and for comparison for future work. Since the P_{id} is dependent *only* on the proximity to the X-ray source and optical magnitude relatively rare objects which are identi-

fied with the USNO A-2 counterpart either by SIMBAD or in other work may be considered as potential counterparts. In this context, "relatively rare" means (roughly) fewer than 1 in 11,301 optical sources at the quoted USNO A-2 magnitude per full sky. We do not list those RASS/BSC sources which only have potential counterparts with $P_{id} < 50\%$ from this analysis.

In Figure 6, we show the distributions of USNO A-2 B and r (RASS/BSC X-ray source–USNO A-2 source separation) for the $P_{id} \geq 98\%$, the 90% Supplementary Catalog and 50% Supplementary Catalog. The $P_{id} \geq 98\%$ sources are largely limited to saturated and $B < 12$ magnitude, while the greatest number of 90% Supplementary sources are between 11 and 14 mag. In positional certainty, the catalog of lesser likelihood has counterparts which are, on average, more distant than the closer such counterparts; even so, more than 90% of the found associations are within 16″.

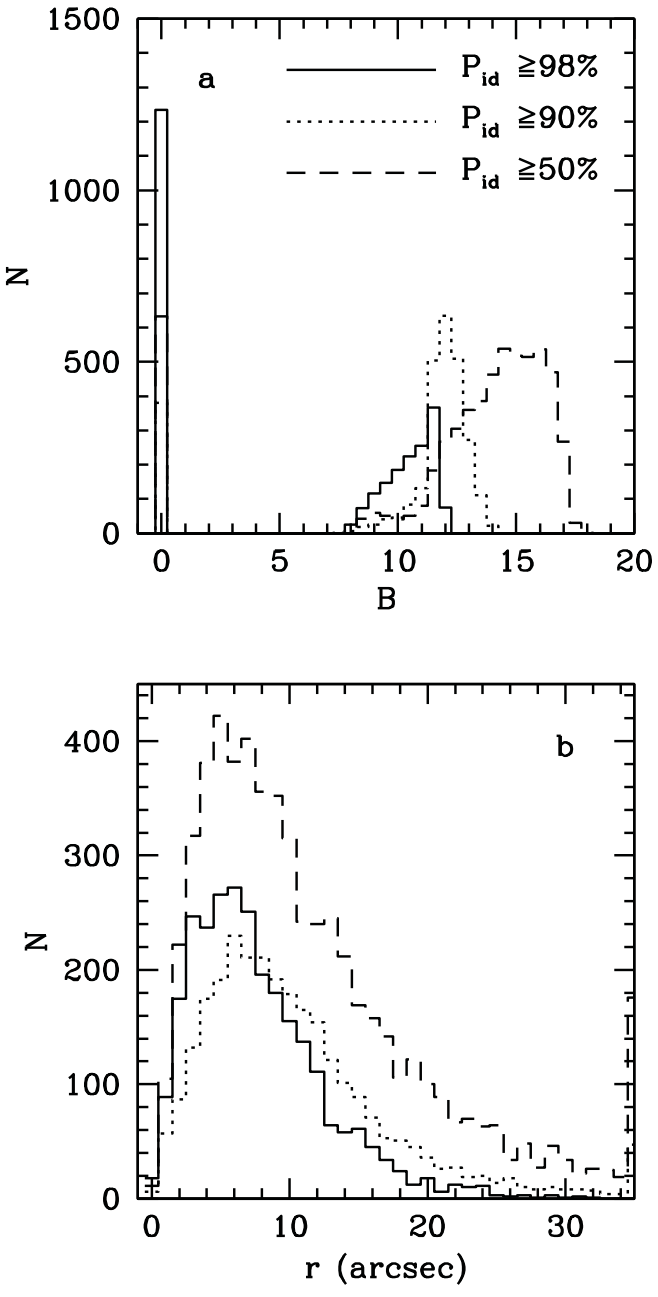

FIG. 6.—Observed B (*a*) distribution and r (*b*) (distance between X-ray source position and the associated counterpart position) for the $P_{id} \geq 98\%$ catalog (*solid line*), the ≥90% Supplementary (*dotted line*) and ≥50% Supplementary Catalogs. The 98% sources are all $B < 12.5$, the 90% extend down to $B = 14$, and the 50% sources all the way down to $B = 17$. The average X-ray/optical source separations are 7.″4 (std. dev. 4.″6) and 10.″3 (std. dev. 7.″0) and 11.9 (std. dev. 9.″2) for the 98% catalog, and 90% and 50% Supplementary catalogs, respectively.

In Figure 7 is the distribution of formal statistical uncertainties in the P_{id} values, for sources with $P_{id} > 0.9$, and sources with $0.9 > P_{id} > 0.5$. The high probability sources ($P_{id} > 0.9$) have an absolute uncertainty of less than 0.01 for 95% of the sources, and less than 0.004 for 65% of the sources. This means the sources identified with $P_{id} \geq 0.98$ are distinguished from sources of lower P_{id} with approximately 0.005 resolution. Objects with lower significance ($0.9 > P_{id} > 0.5$) mostly have absolute uncertainties in the 0.01–0.03 range.

3.2. *Binary Counterparts*

Before excluding RASS/BSC objects which already have counterparts in the single-source catalogs, we found 317, 619, and 3550 binary counterparts in $P_{id} \geq 98\%$, $98\% > P_{id} \geq 90\%$, and $90\% > P_{id} \geq 50\%$, respectively. After excluding, we are left with 6, 25, and 441, respectively, for a total of 472 new associations.

Five out of six of the 98% sources are listed as binaries or cluster members in the SIMBAD database, the exception being the USNO A-2 identifications of 1RXS J041003.0+863735, which are a pair of stars of nearly equal magnitude ($B = 11.4, 11.5$), separated by 5″; the sole nearby optical source in SIMBAD is listed as a single F5 IV star (HD 22701), with $B = 6.2$.

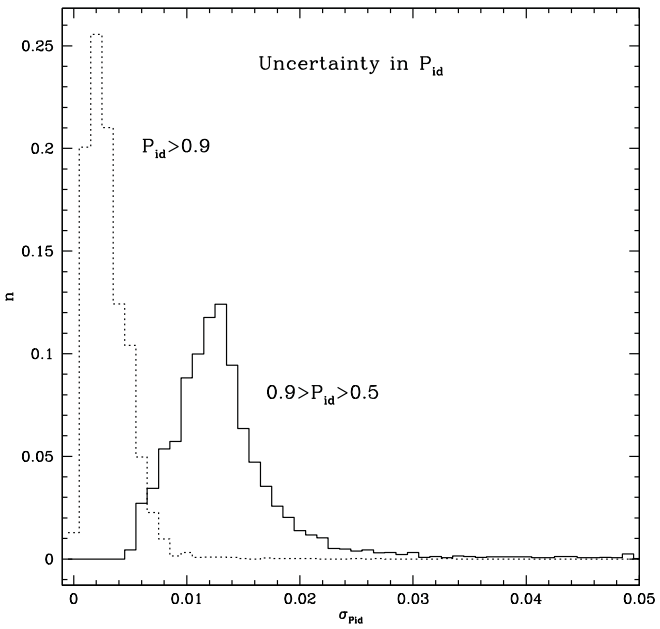

FIG. 7.—The distributions of uncertainty in P_{id} due to the uncertainty in the number of background sources, for sources with $P_{id} > 0.90$ (*dotted line*) and $0.90 > P_{id} > 0.50$ (*solid line*). The small median value of these uncertainties for $P_{id} > 0.90$ makes the distinction between $P_{id} > 0.98$ sources and $P_{id} > 0.90$ a meaningful one. These uncertainties are, essentially, the resolution of P_{id} in the indicated P_{id} ranges.

Inspection of Digital Sky Survey[3] images of a few randomly selected optical sources identified as a binary association reveals that some do not appear as convincing binaries at all, but may have been split into two by the scanning/detection algorithm of USNO A-2. However, while the association itself may not be a binary source, such objects still indicate a significant association, at the quoted P_{id} level, as USNO A-2 should contain as many such false splits in background fields as in on-source fields. Thus, the lists of "binary" counterparts should not be taken to imply that the identified optical binary pair are a physical binary, or even a pair of related objects; it only implies that USNO A-2 scanning/detection algorithm split the plate scan into two objects and that our method finds that the presence of these two objects in the RASS/BSC field is statistically unlikely by serendipity alone. This does, however, require that USNO A-2 magnitudes be viewed critically.

3.3. *Multiplet Counterparts*

We found an average value $\langle 1 - S \rangle = 0.272$ (see § 2.2), which indicates that $\sim$27.2% of the RASS/BSC X-ray sources do not satisfy the unique association/no unique association hypothesis. Alternative hypotheses to explain these sources include multiplet (double, triple, or more) counterparts, where more than one USNO A-2 object is associated with the X-ray source.

3.4. *What Fraction of the RASS/BSC Sources have USNO A-2 Counterparts?*

We find a value of $Q = 65.2\%$ (eq. [7]), which means that (on average) 34.8% of the RASS/BSC X-ray sources have no optical counterparts in the USNO A-2 catalog. This number might be affected by our method of setting $R = 0$ for all $LR < LR_0$, where LR_0 is the highest LR value where $R = 0$. To derive an upper limit to the fraction of RASS/BSC X-ray sources which have counterparts in the USNO A-2 catalog, we reperformed the analysis, instead setting all values of $R = 3\sigma_R$ for all $LR < LR_0$. The exact value of σ_R depends on the number of objects in each LR bin, but it is in all cases ≤ 0.03; from this, we place a 3 σ upper limit on the fraction of RASS/BSC X-ray sources with optical counterparts in the USNO A-2 Catalog identifiable through the present method (searching for bright, nearby sources) at $Q \leq 72.2\%$.

For a limit of $B = 19$, with a corresponding flux of 1.6×10^{-13} ergs cm^{-2} s^{-1} (assuming a flat spectrum; Zombeck 1982) for the USNO A-2 and assuming a value of $F_X = 5 \times 10^{-13}$ ergs cm^{-2} s^{-1} per RASS counts s^{-1} (cf. V99) at the limit of the RASS/BSC catalog, this is a limit of $F_X/F_{opt} \approx 3$. This limit is comparable to values obtained from AGNs, galaxies, and clusters (cf. Fig. 13 of V99) but well above those from stars. Thus, the remaining (unidentified) sources may well be faint extragalactic sources. However, another potential population which may contribute to the unidentified sources are isolated neutron stars (INSs), which have $F_X/F_{opt} \approx 4 \times 10^4$, and it remains an open question what fraction of the RASS/BSC is composed of these objects (two RASS/BSC sources have been identified as INSs; Walter, Wolk, & Neuhauser 1996; Haberl et al. 1997), although a greater number of such objects was expected (Blaes & Madau 1993).

[3] http://archive.stsci.edu/dss/.

4. SOURCE CLASSES

In this section, we briefly discuss the various source classes found in the SIMBAD identifications, using the $P_{id} > 90\%$ Catalog, and the $P_{id} > 50\%$ Catalog. In Table 4, we list the number of each of several source classifications listed in SIMBAD, found within 10″ of these USNO A-2 counterparts. By far, the greatest number of sources here are "unclassified"; these are USNO A-2 objects for which there is no source listed in the SIMBAD database within 10″ of the USNO A-2 position.

4.1. *Chromospherically Active Systems: RS CVn*

In the $P_{id} > 90\%$ Catalog, there are 116 identified counterparts which have been previously classified as RS CVns-like systems (including GJ 501.1 = RS CVn itself). This compares to the study of Dempsey et al. (1993), reporting on detections of 112 RS CVns in the full RASS, in which the X-ray counterparts were found for the optically selected catalog (optical selection); whereas we find them by searching for the bright optical counterpart (X-ray selection). When we include the full $P_{id} \geq 50\%$ catalog, we find 131 RS CVns. This is a substantial fraction of the 162 RS CVns listed in the SIMBAD database.

4.2. *T Tauri Stars*

Of 775 T Tauri stars classified as such in the SIMBAD database, 137 are identified with $P_{id} > 90\%$ with a RASS/BSC source, and 198 are identified with $P_{id} > 50\%$.

4.3. *AGNs and QSOs*

There are a greater fraction of extragalactic objects (AGNs, Quasars, Seyferts, and BL Lacs) in the $P_{id} > 50\%$ Catalog than the $P_{id} > 90\%$ Catalog, likely due to the relative optical faintness of these objects compared to Galactic objects.

4.4. *Unclassified Sources in the $P_{id} > 90\%$ Catalog*

USNO A-2 objects which do not have an entry in SIMBAD within 10″ (which we call "unclassified") make

TABLE 4

SIMBAD Source Types in the $P_{id} > 90\%$ Catalog

Class	N ($P_{id} > 90\%$ Cat.)	N ($P_{id} > 50\%$ Cat.)
Algol	45	61
RS CVn	116	131
W UMa	26	37
T Tauri	137	198
Symbiotic Stars	2	2
White Dwarfs	14	57
Dwarf Novae	9	33
Cataclysm. Var.	7	24
AGN	9	58
Quasar	14	375
Seyferts (1/2)	131	287
BL Lac	7	76
Unclassified	1362	4600

up 25% of the >90% Catalog (1362 objects), and 41% (4600 objects) of the >50% Catalog. A spot check of some of the brightest such objects reveals that a large fraction of these objects are likely to be high proper motion stars, or objects for which the astrometry and SIMBAD positions are different by more than 10″, although some do appear to be objects which were previously not cataloged and classified.

In Figure 8, we show the X-ray count rate distribution and USNO A-2 *B*-magnitude distribution of these sources. The X-ray count rate distribution, compared with distribution of the full RASS/BSC catalog, shows that the unclassified sources tend slightly to be among the fainter objects, although not exclusively so.

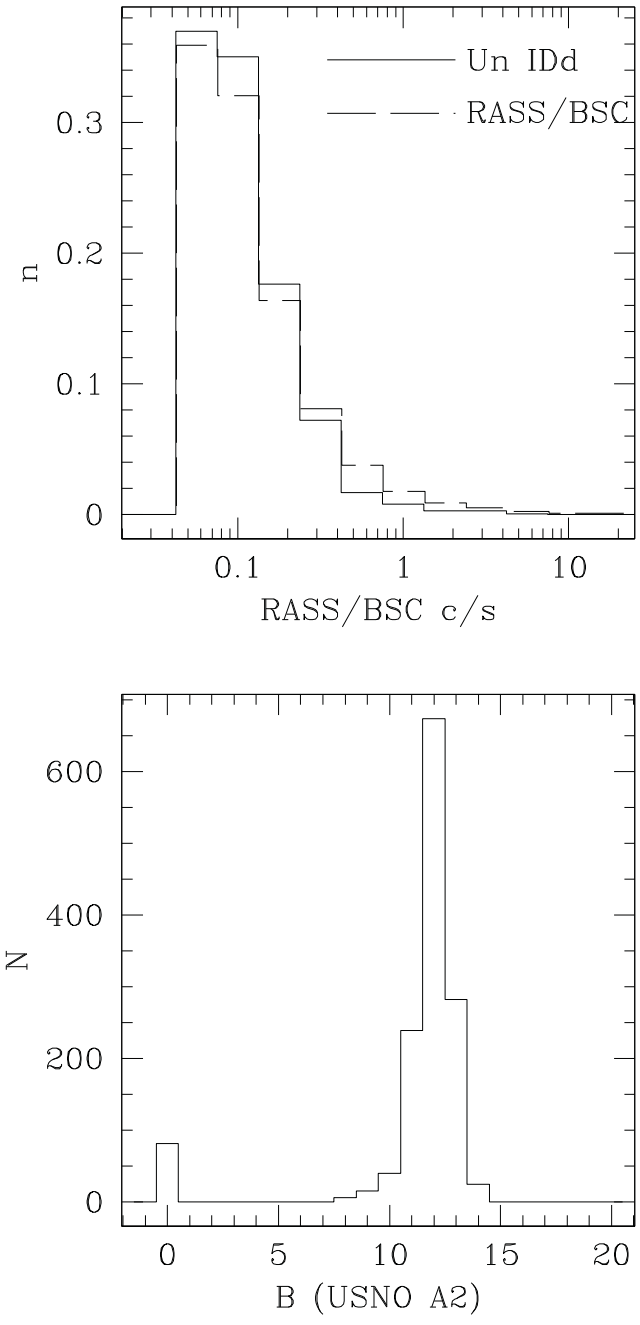

FIG. 8.—*Top*: RASS/BSC count rate distribution of unidentified sources (see text) and all RASS/BSC objects. There is a tendency for the unidentified sources to be among the fainter objects, although this is not strong. *Bottom*: *B* magnitude distribution of the unidentified sources.

5. COMPARISON WITH OTHER PUBLISHED CROSS-IDENTIFICATION CATALOGS

The $P_{id} > 50\%$ catalog is between 2 and 10 times greater in size of other published catalogs with similar limiting P_{id} (Table 1), with the exception of V99, for which we provide a more detailed comparison below. However, we note that previous work has used what we define as R as their catalog probability limit, whereas we use P_{id}, which is always less than or equal to R. For example, while we find 11,301 sources with $P_{id} \geq 50\%$, we find 12,462 sources with $R \geq 50\%$.

V99 presented results of cross-identifications with 16 different catalogs of various types of sources (optical, radio). In the largest such comparison, they describe cross-identifications with the *Hubble Space Telescope* Guide Star Catalog (*HST*-GSC; Lasker et al. 1990; Russell et al. 1990; Jenkner et al. 1990; Taff et al. 1990), for which $R = 50\%$ at a distance $\sim 24''$ from the RASS-BSC position than expected from (the background) source density extrapolation from further away (40″–60″); further, this extrapolation indicated that 13.92% of the 15,824 *HST*-GSC objects within 24″ of RASS/BSC X-ray sources were background sources, with the remainder being associated with the RASS/BSC X-ray source. Of the *HST*-GSC objects, 9759 were the sole object in the 24″ field, making them unique identifications down to $P_{id} = 50\%$, with a contamination rate of 13.92%. In the remaining 6056 fields, multiple objects either indicate an association with clustered sources (galaxies, stars), or confusion in the true, unique association. The *HST*-GSC results of V99 are consistent the results of the present work (11,301 objects, to $P_{id} = 50\%$, contamination rate of 18%).

In addition, comparisons with many different cross-identification catalogs were performed by V99 (NVSS, Tycho, *FIRST*, *EUVE*, and *IRAS*, for example), and the primary statistical result for each catalog was a search radius, at which $R = 50\%$ (W. Voges 1999, private communication), using exclusively spatial proximity. In these comparisons, V99 found 17,017 possible counterparts within 90″ of the RASS/BSC position, 7117 of which are the sole object in the 90″ region. As with the *HST*-GSC results, a search radius was found for each catalog at which $P_{id} = 50\%$. The number of candidate objects within the search radius, the estimated background source contamination, and the search radius itself varies from catalog to catalog.

V99 associations are made exclusively on proximity between the cross-ID and the RASS/BSC source (the closest object is the most likely counterpart). In contrast, the algorithm in the present work also makes use of *B*-band brightness. Thus, a brighter *B*-band object which is further from the RASS/BSC source from a fainter *B*-band object can be identified as a counterpart (if bright enough). On the other hand, objects which have unusually *high B* magnitude would be considered highly unlikely counterparts in the present work (cf. eq. [2]), while in V99, they may be considered a possible counterpart on the basis of spatial proximity alone. In the present work, we have evaluated a unique likelihood of association (P_{id}) for each object, while individual object P_{id}-values are not available in V99. Thus, while the present and V99 catalogs are similar in size, future work based on the present catalog can select out high-

TABLE 5

NUMBER OF IDENTIFIED OPTICAL COUNTERPARTS

P_{id}	N (Single ID)[a]	N (Binary ID)[b]	N ("Blank" Fields)[c]	Totals
$\geq 98\%$	2705	6	30	2741
$98 > P_{id} \geq 90\%$.....	2787	25	...	2812
$90 > P_{id} \geq 50\%$.....	5809	441	...	6252
Total.....	11301	472	30	11803

[a] See § 3.1.
[b] See § 3.2.
[c] See § 3.

quality identifications for targeted work or draw more broadly upon the lower quality identifications for statistical studies based on the unique P_{id} for each counterpart.

6. CATALOG ACCESS AND CONTENTS

The four catalogs, given in the Appendix, contain: (1) a list of the *ROSAT*/BSC object by name; (2) the RASS/BSC count rate and uncertainty; (3) the P_{id} with the identified USNO A-2 counterpart; (4) the USNO A-2 *B* magnitude; (5) USNO A-2 name/position (hhmmss.ss+−ddmmss.s J2000); (6) the name of SIMBAD objects within 10″ of the USNO A-2 source; (7) the source classification listed in SIMBAD for these objects (variable star, binary system, galaxy, etc.); (8) the source type listed in SIMBAD (stellar spectral type or galaxy type); (9) SIMBAD *B* and *V* magnitudes; and (10) accompanying source notes, including a flag if that SIMBAD object was previously identified as the RASS/BSC source. If there are more than one SIMBAD objects within 10″ of the USNO A-2 source, these are listed on subsequent lines. It is not implied that the SIMBAD objects *are* the USNO A-2 counterpart, although we expect this to often be the case, as can be told by comparing the USNO A-2 *B* magnitude to that reported by SIMBAD. The SIMBAD objects are listed to suggest them as the USNO A-2 counterpart, or to at least potentially provide information about the counterpart's environment (such as in a cluster of galaxies, or a stellar cluster).

7. DISCUSSION AND CONCLUSIONS

We have cross-correlated the 18,811 RASS/BSC X-ray sources with 321,144 candidate USNO A-2 optical counterparts within 75″ of the RASS/BSC source position, on the basis of *B* magnitude and source proximity, taking into account the quoted RASS/BSC positional uncertainty. On this basis, we identify 2705 USNO A-2 objects with $P_{id} > 98\%$, with $\sim 0.66\%$ background contamination; 5492 with $P_{id} > 90\%$, with $\sim 2.8\%$ background contamination; and 11,301 with $P_{id} > 50\%$, with $\sim 18\%$ background contamination. Thus, we have identified possible optical counterparts to 60% of the *ROSAT*/BSC on the basis of position and photometry alone. We have also provided—for the first time—a probability of unique identification between each of the X-ray sources and their proposed counterpart. When we include unique "binary" identifications, and 30 high-surface brightness objects which were not included in USNO A-2, we have presented optical associations for a total of 11,803 objects, down to a limiting identification probability of 50%, which is 62.7% of the RASS/BSC catalog objects. More conservatively, we have presented optical associations for 5553 objects, to $P_{id} \geq 90\%$, which is 29.5% of the RASS/BSC catalog. The breakdown of these identified sources is listed in Table 5.

The individual identifications are subject to systematic uncertainty of the association between X-ray sources and clustered optical sources (such as clusters of galaxies, open stellar clusters and star formation regions), in which the X-ray source may reside, and the greater than average density of candidate optical counterparts makes the presence of a brighter-than-average source more likely than in a background field. Thus, the given optical identification should be considered an "association"—and the likelihood that the source of X-ray emission is the identified optical point source directly or a nearby associated object must be evaluated on a case-by-case basis, on the basis of the likelihood of such a secondary association.

For these sources, we have listed the RASS/BSC source name, and the identified USNO A-2 counterpart. In addition, we compiled a list of objects in the SIMBAD database within 10″ of the USNO A-2 counterpart, many of which are likely to be the USNO A-2 counterpart itself. There are a surprisingly high fraction (25% in the $P_{id} > 90\%$ Catalog) of optical counterparts which are not named in the SIMBAD database. As these are (photometrically) identical to objects which have been previously classified, the unclassified objects are likely to be the same population. Thus, a program of classification of these unclassified objects will likely discover new examples of known classes of sources, although they may contain unknown classes as well.

The limit on the fraction of RASS/BSC sources which have counterparts in the USNO A-2 catalog discoverable by this method is $Q \leq 72.2\%$. To improve this identification fraction between X-ray sources and optical data, either additional optical information is required (source classes, spectral colors) which will help distinguish identifiable sources, or improved X-ray localizations (such as from the *ROSAT*/HRI, or *Chandra*), or combining X-ray and optical information to pick out sources of particular classes (L_X/L_{opt}).

The authors are grateful to the anonymous referee for careful reading of the manuscript. This paper was produced under the Digital Sky Project of the NPACI program (NSF Cooperative Agreement ACI-96-19020) and NASA grant NAG5-3239. This research has made use of the SIMBAD database, operated at CDS, Strasbourg, France. This research has made use of the NASA/IPAC Extragalactic Database (NED) which is operated by the Jet Propulsion Laboratory, California Institute of Technology, under contract with the National Aeronautics and Space Administration.

APPENDIX

TABLES OF CROSS-IDENTIFICATIONS BETWEEN THE *ROSAT*/BRIGHT SOURCE CATALOG AND USNO-A2 CATALOGS

Tables 6, 7, and 8 describe the format and values in Tables 9, 10, 11, and 12.

In Table 12, the magnitudes and USNO A-2 designations of the two sources are separated by a backslash. Please be aware of the points of caution regarding the "Optical Pairs" counterparts. In column (7), the source types are often abbreviated according to the scheme in Table 8, which closely follows the source types used by SIMBAD.

Additional lines are given for each SIMBAD object within 10″ of the USNO A-2 counterpart (20″ for the optical pairs). Note that the counterpart for which the P_{id} applies is the USNO A-2 counterpart; the SIMBAD identifications are listed to provide *possible* identifications of this source. The SIMBAD B and V magnitudes provide a point of comparison with the USNO A-2 B magnitude which may help in identifying the USNO A-2 object, however the USNO A-2 B magnitudes are subject to certain systematic errors and should be viewed with caution. Column (10) holds comment codes of which, at present, there is only one: P = SIMBAD object has been previously identified as this RASS/BSC source.

TABLE 6

APPENDIX TABLE CONTENTS

Table	Content	From Section	Number of Objects
9.....	$P_{id} \geq 98\%$	3.1	2705
10.....	$98\% > P_{id} \geq 90\%$	3.1	2787
11.....	$90\% > P_{id} \geq 50\%$	3.1	5809
12.....	Optical Pairs $P_{id} \geq 50\%$	3.2	472

TABLE 7

COLUMN DESCRIPTIONS

Column	Heading	Description
1.....	1RXS	The *ROSAT*/BSC Name for the X-ray source
2.....	PSPC c/s (σ)	RASS/BSC Catalog X-ray count rate and 1 σ uncertainty
3.....	P_{id}	Calculated fractional probability of unique association between the X-ray and USNO A-2 objects
4.....	B_{USNOA2}	The USNO A-2 B magnitude
5.....	USNO A2	The USNO A-2 source name/position (hhmmss.ss $\pm$ ddmmss.s)
6.....	SIMBAD crossID	List of all objects $<10''$from the USNO A-2 position
7.....	Type	SIMBAD object population
8.....	Class	Classification of the SIMBAD object
9.....	B:V	SIMBAD B and V magnitudes
10	Comments	Comment code

TABLE 8

SOURCE TYPES

Abbreviation	Meaning	Abbreviation	Meaning	Abbreviation	Meaning
*	Star	HiPM*	High proper-motion star	SN	Supernova
**	Stellar binary	HMXB	High-mass X-ray binary	Spec. Bin.....	Spectroscopic binary
*iC	Star in cluster	IR	Infrared object	Sy1	Seyfert 1
**mul	Multiple stellar system	Glob. Clust.....	Globular cluster	Sy2	Seyfert 2
*Neb	Star in nebula	Gal.	Galaxy	TT	T-Tauri type star
Clust.....	Cluster	GiG.....	Galaxy in group of galaxies	UV	Ultraviolet emission source
CV	Cataclysmic variable	LMXB	Low-mass X-ray binary	V*	Variable star
Ceph.....	Cepheid variable	LSBG	Low Surface Brightness Galaxy	WD	White dwarf
DN	Dwarf nova	PN	Planetary Nebula	WR *	Wolf-Rayet star
Ecl. Bin.....	Eclipsing binary (and type)	Rad.	Radio source	X	X-ray source
Em. *.....	Emission line star	Rot. Var. *.....	Rotationally variable star	YSO	Young stellar object

TABLE 9

CATALOG OF RASS/BSC-USNO A-2 ASSOCIATIONS, WITH $P_{id} \geq 98\%$, AND SIMBAD SOURCES WIHTIN 10′

1RXS	PSPC c/s (σ)	P_{id}	B_{USNOA2}	USNOA2	SIMBAD CrossID	Type	Class	B:V	Comments
1RXSJ000042.5+621034.....	0.1592 (0.0186)	0.999	0.0	000041.64+621033.2	HD 224792	*	G0	7.532:7.060	
1RXSJ000226.6+032105.....	0.2263 (0.0267)	0.998	10.4	000226.47+032106.9	NGC 7811	Sy1	S0	14.9:	P
1RXSJ000256.6+712207.....	0.0847 (0.0139)	0.986	11.7	000256.67+712204.6	CCDM J00029+7122B	**	K0	10.43:9.20	
1RXSJ000259.6+395743.....	0.0567 (0.0148)	0.990	8.9	000258.47+395741.9	HD 225055	*	A	8.91:8.91	
1RXSJ000442.5+170422.....	0.0694 (0.0149)	0.996	9.3	000442.52+170411.9	HD 225240	*	G5	9.34:8.58	
1RXSJ000539.8−075407.....	0.1407 (0.0224)	0.987	11.4	000539.68−075413.2	HD 74	*	K0	10.51:9.62	
1RXSJ000552.5−414521.....	0.1482 (0.0316)	0.998	0.0	000552.55−414511.1	HD 105	*	G0V	8.13:7.53	P
1RXSJ000636.8+290112.....	0.6868 (0.0484)	0.998	0.0	000636.78+290117.4	GJ 5	V*	K0V	6.88:	P
1RXSJ000724.1−423331.....	0.0874 (0.0254)	0.999	0.0	000724.05−423336.5	HD 271	*	F5/F6V	9.97:9.55	
1RXSJ000751.8+553446.....	0.0574 (0.0128)	0.998	8.4	000751.00+553436.6	HD 299	HiPM*	G0	8.5:7.8	
1RXSJ000802.4+534755.....	0.0580 (0.0131)	0.988	8.9	000804.37+534748.4	HD 330	*	F8	8.72:8.16	
1RXSJ000910.1+590903.....	0.1625 (0.0195)	1.000	0.0	000910.09+590900.8	GJ 8	V* (delta Sct)	F2IV	2.61:2.27	P
1RXSJ001002.8+110845.....	0.1873 (0.0196)	0.999	0.0	001002.20+110844.9	HD 560	**	B9Vn	5.473:5.537	P
.....	...	...	...	001002.20+110844.9	HD 560 B	**	G5Ve	:	
1RXSJ001229.4+143358.....	1.0380 (0.0636)	0.998	9.7	001229.23+143352.0	...	...	...	...	
1RXSJ001309.6+053550.....	0.4236 (0.0327)	0.983	12.1	001309.56+053552.2	...	...	...	...	
1RXSJ001337.6+770210.....	0.1004 (0.0114)	0.984	11.5	001340.17+770210.9	GSC 04496−00780	*	./.	10.36:9.76	
1RXSJ001354.6−744122.....	0.5177 (0.0386)	0.999	0.0	001353.02−744117.8	GSPC S 28−B	*	./.	9.54:8.80	
.....	...	...	...	001353.02−744117.8	HD 987	**	G6V	9.46:8.74	
1RXSJ001420.2+261630.....	0.0786 (0.0186)	0.997	9.7	001420.11+261622.4	BD+25 19	*	G0	9.66:9.04	

NOTE.—Table 9 is published in its entirety in the electronic edition of *The Astrophysical Journal*. A portion is shown here for guidance regarding its form and content.

TABLE 10

SUPPLEMENTARY 90% RASS/BSC ASSOCIATIONS IN USNO CATALOG, AND SIMBAD SOURCES WITHIN 10″

1RXS	PSPC c/s (σ)	P_{id}	B_{USNOA2}	USNOA2	SIMBAD CrossID	Type	Class	B:V	Comments
1RXSJ000007.0+081653.....	0.1869 (0.0205)	0.953	12.6	000007.05+081645.5	PMN J0000+0816	Rad.	./.	:	
.....	...	...	...	000007.05+081645.5	[HDL96] 408 15	Gal.	E	16.0:	P
1RXSJ000013.5+575628.....	0.1178 (0.0173)	0.959	12.1	000013.35+575639.1	...	...	...	...	
1RXSJ000038.4+794037.....	0.1007 (0.0127)	0.973	11.4	000040.85+794040.0	BD+78 853	*	G	10.95:10.28	
1RXSJ000143.9+521246.....	0.0836 (0.0148)	0.976	11.4	000142.67+521252.8	HD 236278	*	G5	10.03:9.30	
1RXSJ000232.0+184125.....	0.0541 (0.0140)	0.970	8.6	000233.47+184059.7	HD 225000	*	F5	8.68:8.25	
1RXSJ000307.6−180550.....	0.3185 (0.0343)	0.978	11.8	000307.86−180549.9	...	...	...	...	
1RXSJ000308.6+215728.....	0.0964 (0.0197)	0.931	10.8	000309.65+215737.7	UGC 6	Sy1	Sc	14.62:	P
1RXSJ000453.0+343934.....	0.6285 (0.0519)	0.968	11.6	000453.81+343931.1	GJ 3002	HiPM*	G2V	6.74:6.10	P
1RXSJ000519.1−293004.....	0.0555 (0.0159)	0.971	11.8	000518.37−293005.8	CD−30 19826	*iC	./.	9.9:	
1RXSJ000543.1−500703.....	0.3794 (0.0696)	0.928	12.9	000543.06−500654.7	DRCG 0003−50	Clust.	./.	:	
.....	...	...	...	000543.06−500654.7	[D80] DRCG 0003−50 66	Sy1	S0	14.:	
1RXSJ000605.0+634039.....	0.0614 (0.0124)	0.955	12.1	000603.51+634046.3	HD 108	Em. *	O6pe	7.494:7.382	
1RXSJ000618.9+201215.....	2.4820 (0.0973)	0.926	12.6	000619.53+201210.7	QSO 0003+199	Sy1	S...	14.19:13.85	P
1RXSJ000637.5+552717.....	0.0929 (0.0153)	0.979	11.6	000637.47+552722.0	HD 232102	*	K0	10.28:9.37	
1RXSJ000714.2−103634.....	0.0618 (0.0161)	0.924	13.0	000714.25−103626.7	...	...	...	...	
1RXSJ000732.4+331730.....	2.0980 (0.0799)	0.938	13.6	000732.53+331730.3	GD 2	WD	DAw...	13.53:13.82	P
1RXSJ000818.4+512319.....	0.9607 (0.0459)	0.926	13.5	000818.03+512316.8	...	...	...	...	
1RXSJ000827.2−405137.....	0.0898 (0.0236)	0.958	11.5	000827.07−405127.2	...	...	...	...	
1RXSJ000849.3+455316.....	0.0866 (0.0159)	0.945	12.9	000849.21+455315.5	EF B0006+4535	Rad.	./.	:	

NOTE.—Table 10 is published in its entirety in the electronic edition of *The Astrophysical Journal*. A portion is shown here for guidance regarding its form and content.

TABLE 11

SUPPLEMENTARY 50% RASS/BSC ASSOCIATIONS IN USNO CATALOG, AND SIMBAD SOURCES WITHIN 10″

1RXS	PSPC c/s (σ)	P_{id}	B_{USNOA2}	USNOA2	SIMBAD CrossID	Type	Class	B:V	Comments
1RXSJ000011.9+052318.....	0.2637 (0.0258)	0.738	15.8	000011.74+052317.5	1RXS J000011.9+052318	Sy1	./.	16.4:	P
1RXSJ000012.6+014621.....	0.0811 (0.0161)	0.734	0.0	000012.20+014617.4	HD 224725	**mul.	G0	10.45:9.81	
1RXSJ000044.2−260521.....	0.1147 (0.0222)	0.556	15.2	000043.92−260521.8	...	...	...	...	
1RXSJ000115.6+705535.....	0.0685 (0.0142)	0.886	8.4	000117.63+705538.0	HD 224854	*	F0	8.13:7.73	
1RXSJ000123.3+272241.....	0.0655 (0.0159)	0.578	16.0	000123.52+272241.7	...	...	...	...	
1RXSJ000154.2−670749.....	0.2415 (0.0301)	0.741	14.8	000155.08−670743.6	...	...	...	...	
1RXSJ000209.4+672503.....	0.0975 (0.0168)	0.560	0.0	000210.29+672432.2	BD+66 1675	*iC	O7	10.04:9.08	
1RXSJ000231.0+082931.....	0.0770 (0.0156)	0.809	11.4	000230.01+082908.4	HD 225003	*	F0V	5.989:5.705	
1RXSJ000312.3−355541.....	0.5206 (0.0583)	0.636	13.9	000312.97−355613.3	ESO 349− 22	Gal.	S0	15.:	P
1RXSJ000316.8−275627.....	0.1132 (0.0218)	0.588	16.2	000316.83−275627.0	...	...	...	...	
1RXSJ000359.1+433600.....	0.3201 (0.0316)	0.684	15.7	000358.62+433602.8	...	...	...	...	
1RXSJ000419.5−642517.....	0.0812 (0.0197)	0.617	14.2	000415.70−642525.3	...	...	...	...	
1RXSJ000454.0−290929.....	0.0542 (0.0150)	0.781	13.0	000454.07−290911.1	...	...	...	...	
1RXSJ000513.2−625050.....	0.0637 (0.0188)	0.737	0.0	000509.80−625042.8	HD 24	*	G0V	8.69:8.14	
1RXSJ000521.2−742632.....	0.3614 (0.0317)	0.586	15.9	000520.44−742640.2	2E 0002.8−7443	X	./.	16.3:	P
1RXSJ000547.7+020306.....	0.2229 (0.0297)	0.547	16.9	000547.54+020302.6	[VV96] J000547.5+020302	Quasar	./.	17.:16.6	P
1RXSJ000549.4+543319.....	0.0559 (0.0121)	0.697	14.8	000549.15+543321.8	...	...	...	...	
1RXSJ000556.1−203850.....	0.0554 (0.0173)	0.794	10.8	000557.45−203854.4	BD−21 6532A	*	./.	10.97:10.34	
1RXSJ000559.1+160955.....	0.3404 (0.0267)	0.674	15.8	000559.24+160949.0	[VV96] J000559.3+160949	Quasar	?	16.51:	P
1RXSJ000604.7−344349.....	0.2485 (0.0368)	0.780	11.8	000602.49−344405.9	...	...	...	...	

NOTE.—Table 11 is published in its entirety in the electronic edition of *The Astrophysical Journal*. A portion is shown here for guidance regarding its form and content.

TABLE 12

RASS/BSC Cross IDs with Paired USNO A-2 Objects

1RXS	PSPC c/s (σ)	P_{id}	B_{USNOA2}	USNOA2	SIMBAD CrossID	Type	Class	B:V	Comments
1RXSJ000202.5−103030…	0.0609 (0.0162)	0.596	16.9/15.4	000202.09−103022.8/000202.96−103037.9	…	…	…	…	
1RXSJ000813.3−005752…	0.0507 (0.0135)	0.698	15.8/17.7	000812.21−005756.2/000813.25−005753.3	…	…	…	…	
1RXSJ001000.6+490655…	0.0506 (0.0133)	0.559	16.5/16.0	001000.08+490638.9/001001.35+490659.0	…	…	…	…	
1RXSJ001049.7−081717…	0.1019 (0.0194)	0.808	13.6/16.3	001049.14−081651.6/001049.60−081722.2	PHL 2695	Blue object	./.	18.5:	
1RXSJ001248.7−084705…	0.1232 (0.0214)	0.569	16.2/16.3	001247.92−084700.3/001248.60−084644.4	…	…	…	…	
1RXSJ001454.6−155215…	0.0535 (0.0151)	0.713	17.3/17.0	001454.84−155213.4/001454.97−155208.9	…	…	…	…	
1RXSJ002158.0+491245…	0.0737 (0.0142)	0.529	14.4/17.1	002156.87+491239.6/002158.17+491243.1	GJ 3030	*	M2.5	:	
1RXSJ002605.4−185456…	0.1336 (0.0242)	0.685	15.0/15.0	002604.91−185453.0/002605.56−185454.2	…	…	…	…	
1RXSJ002636.3−460101…	0.8940 (0.0752)	0.784	17.2/15.9	002635.62−460110.0/002636.59−460052.2	1RXS J002636.3-460101	X	B...	:	P
1RXSJ002816.2−354212…	0.1960 (0.0271)	0.534	16.8/16.5	002815.52−354205.5/002815.59−354155.1	…	…	…	…	
1RXSJ003057.5−655020…	0.0653 (0.0197)	0.628	15.1/11.9	003057.63−655005.5/003101.66−654943.9	…	…	…	…	
1RXSJ003224.5+065742…	0.3972 (0.0577)	0.989	0.0/0.0	003223.77+065719.6/003225.58+065723.0	ADS 449 AB	**mul.	?	5.66:5.66	
……	…	…	…	003223.77+065719.6/003225.58+065723.0	HD 2913	**	B9.5V	5.683:5.698	
1RXSJ003400.0−384718…	0.0978 (0.0207)	0.890	15.2/14.8	003359.17−384716.4/003401.16−384725.5	CTS 32	Sy1	./.	:	P
1RXSJ003528.6+603139…	0.0858 (0.0190)	0.579	17.4/14.7	003528.20+603133.9/003529.98+603128.5	…	…	…	…	
1RXSJ003956.6−175003…	0.0810 (0.0180)	0.550	16.3/15.4	003956.64−174940.2/003956.82−175024.5	…	…	…	…	
1RXSJ004044.3−344006…	0.2553 (0.0299)	0.562	16.7/18.8	004043.97−343956.8/004044.13−344014.1	HBQS 0038-3456	HII (ionized) region	./.	17.29:	
1RXSJ004400.0+313729…	0.0521 (0.0143)	0.673	16.6/14.8	004359.86+313720.4/004359.98+313704.5	RX J0043.9+3137	Quasar	./.	:	P
1RXSJ004501.2+793054…	0.0531 (0.0099)	0.617	13.7/14.6	004509.07+793109.8/004509.35+793036.3	…	…	…	…	
1RXSJ004704.9+031959…	0.0602 (0.0156)	0.613	15.5/16.2	004705.94+031954.1/004706.07+031947.8	[VV96] J004705.9+031955	Quasar	./.	16.2:16.3	P

Note.—Table 12 is published in its entirety in the electronic edition of *The Astrophysical Journal*. A portion is shown here for guidance regarding its form and content.

REFERENCES

Bade, N., et al. 1998, A&AS, 127, 145
Bade, N., Fink, H. H., Engels, D., Voges, W., Hagen, H. J., Wisotzki, L., & Reimers, D. 1995, A&AS, 110, 469
Berghoefer, T. W., Schmitt, J. H. M. M., & Cassinelli, J. P. 1996, A&AS, 118, 481 (erratum 121, 212 [1997])
Berghoefer, T. W., Schmitt, J. H. M. M., Danner, R., & Cassinelli, J. P. 1997, A&A, 322, 167
Beuermann, K., Thomas, H. C., Reinsch, K., Schwope, A. D., Trueper, J., & Voges, W. 1999, A&A, 347, 47
Blaes, O., & Madau, P. 1993, ApJ, 403, 690
Dempsey, R. C., Linsky, J. L., Fleming, T. A., & Schmitt, J. H. M. M. 1993, ApJS, 86, 599
Gliese, W., & Jahreiss, H. 1991, in The Astronomical Data Center CD-ROM: Selected Astronomical Catalogs, Vol. I, ed. L. E. Brotzmann & S. E. Gesser (Greenbelt: NASA-Goddard Space Flight Center)
Haberl, F., Motch, C., Buckley, D. A. H., Zickgraf, F. J., & Pietsch, W. 1997, A&A, 326, 662
Hoffleit, D., & Jaschek, C. V. 1991, The Bright Star Catalogue (5th rev ed.; New Haven: Yale Univ. Obs.)
Huensch, M., Schmitt, J. H. M. M., & Voges, W. 1998a, A&AS, 127, 251
———. 1998b, A&AS, 132, 155
Huensch, M., Schmitt, J. H. M. M., Sterzik, M. F., & Voges, W. 1999, A&AS, 135, 319
Jenkner, H., Lasker, B. M., Sturch, C. R., McLean, B. J., Shara, M. M., & Russel, J. L. 1990, AJ, 9, 2082
Lasker, B. M., Sturch, C. R., McLean, B. J., Russell, J. L., Jenkner, H., & Shara, M. M. 1990, AJ, 99, 2019
Lonsdale, C., et al. 1998, in IAU Symp. 179, New Horizons from Multi-Wavelength Sky Surveys, ed. B. J. McClean, D. A. Golombeck, J. J. E. Hayes, & H. E. Payne (Dordrecht: Kluwer), 450
Motch, C., Guillout, P., Haberl, F., Pakull, M. W., Peitsch, W., & Reinsch, K. 1997a, A&AS, 122, 201
Motch, C., Haberl, F., Dennerl, K., Pakull, M., & Janot-Pacheco, E. 1997b, A&A, 323, 853
Russell, J. L., Lasker, B. M., McLean, B. J., Sturch, C. R., & Jenkner, H. 1990, AJ, 99, 2059
Sutherland, W., & Saunders, W. 1992, MNRAS, 259, 413
Taff, L. G., et al. 1990, ApJ, 353, L45
Thomas, H. C., Beuermann, K., Reinsch, K., Schwope, A. D., Truemper, J., & Voges, W. 1998, A&A, 335, 467
Voges, W., et al. 1996, IAU Circ., 6420, 2
Voges, W., et al. 1999, A&A, 349, 389 (V99)
Walter, F. M., Wolk, S. J., & Neuhauser, R. 1996, Nature, 379, 233
Zombeck, M. V. 1982, Handbook of Space Astronomy and Astrophysics (Cambridge: Cambridge Univ. Press)